

# ADVANCED MATERIALS

## Supporting Information

for *Adv. Mater.*, DOI 10.1002/adma.202313991

Manipulating Radiation-Sensitive Z-DNA Conformation for Enhanced Radiotherapy

*Dongmei Wang, You Liao, Hao Zeng, Chenglu Gu, Xue Wang, Shuang Zhu, Xihong Guo, Jie Zhang, Ziye Zheng, Junfang Yan, Fuquan Zhang, Lingmi Hou\*, Zhanjun Gu\* and Baoyun Sun\**

## Supporting Information

### Manipulating Radiation-Sensitive Z-DNA Conformation for Enhanced Radiotherapy

Dongmei Wang<sup>1,4,5</sup>, You Liao<sup>1,4,5</sup>, Hao Zeng<sup>1,4</sup>, Chenglu Gu<sup>1,4</sup>, Xue Wang<sup>1,4</sup>, Shuang Zhu<sup>1</sup>, Xihong Guo<sup>1</sup>, Jie Zhang<sup>3</sup>, Ziyi Zheng<sup>3</sup>, Junfang Yan<sup>3</sup>, Fuquan Zhang<sup>3</sup>, Lingmi Hou<sup>2\*</sup>, Zhanjun Gu<sup>1,4\*</sup>,  
Baoyun Sun<sup>1,4\*</sup>

<sup>1</sup> CAS Key Laboratory for Biomedical Effects of Nanomaterials and Nanosafety, Institute of High Energy Physics, Chinese Academy of Sciences, Beijing 100049, China

<sup>2</sup> Academician (Expert) Workstation, Breast Cancer Biotarget Laboratory, Medical Imaging Key Laboratory of Sichuan Province, Department of Breast and Thyroid Surgery, Affiliated Hospital of North Sichuan Medical College, Nanchong, Sichuan, 637000, China

<sup>3</sup> Department of Radiation Oncology, Peking Union Medical College Hospital, Chinese Academy of Medical Sciences & Peking Union Medical College, Beijing 100730, China

<sup>4</sup> University of Chinese Academy of Sciences, Beijing 100049, China

<sup>5</sup> These authors contributed equally to this work.

\* Corresponding author. E-mail: houlingmi@nsmc.edu.cn (L. Hou); zjgu@ihep.ac.cn (Z. Gu); sunby@ihep.ac.cn (B. Sun).

## Table of Content

<b>Experimental Section</b> .....	<b>4</b>
Characterization .....	4
Cell lines and animals .....	4
Simulated calculation.....	4
Cellular uptake.....	5
<i>In vitro</i> biocompatibility evaluation .....	5
<i>In vivo</i> toxicological evaluation.....	5
<b>Supplementary Figures</b> .....	<b>7</b>
Figure S1   The X-ray mass attenuation coefficients of HfO <sub>2</sub> and soft tissues.....	7
Figure S2   Characterization of SiO <sub>2</sub> as a template.....	8
Figure S3   Synthesis and characterization of CBL@HfO <sub>2</sub> .....	9
Figure S4   The cellular uptake behavior of CBL@HfO <sub>2</sub> after incubating for 8 hours.....	10
Figure S5   Cytotoxicity evaluation with treatments by HM-HfO <sub>2</sub> , CBL0137, and CBL@HfO <sub>2</sub> .....	11
Figure S6   Z-DNA expression within HCT116, A549, MDA-MB-231, HeLa cells.....	12
Figure S7   Comet assay of HCT116 cells with treatment.....	13
Figure S8   The $\gamma$ H2AX expression within HCT116, A549, MDA-MB-231, and HeLa cells.....	14
Figure S9   The $\gamma$ H2AX expression within HCT116, A549, MDA-MB-231, and HeLa cells.....	15
Figure S10   The $\gamma$ H2AX expression within HCT116 cells after different treatments.....	16
Figure S11   The co-staining of $\gamma$ H2AX and Z-DNA within HCT116 cells after treatments.....	17
Figure S12   The Z-DNA expression within HCT116 cells after different doses of irradiation.....	18
Figure S13   The $\gamma$ H2AX and Z-DNA expression within HCT116 cells after treatment with different concentrations of CBL0137.....	19
Figure S14   Colony formation of HCT116 cells treated with HM-HfO <sub>2</sub> , CBL0137, and CBL@HfO <sub>2</sub> .....	20
Figure S15   Cell death evaluation of HCT116 cells after treatments.....	21
Figure S16   Hemolysis assay of HM-HfO <sub>2</sub> , CBL0137, and CBL@HfO <sub>2</sub> .....	22
Figure S17   <i>In vivo</i> toxicological evaluation.....	23
Figure S18   Histologic sections of major organs with intratumoral treatment.....	24
Figure S19   Photographs of mice after treatment at day 30.....	25
Figure S20   Photographs of tumor regression.....	26
Figure S21   Body weight curves of mice with treatments.....	27
Figure S22   Histologic sections of major organs with intratumoral treatment and subsequent IR irradiations.....	28
Figure S23   Expression of H&E in tumor sections.....	29
Figure S24   Damage analysis of tumor and peritumoral normal tissue after CBL@HfO <sub>2</sub> and IR treatment.....	30
Figure S25   <i>In vivo</i> radiosensitization based on CBL@HfO <sub>2</sub> nanocapsule.....	31
Figure S26   The $\gamma$ H2AX and Z-DNA expression within CT26 tumor sections.....	32
Figure S27   Developmental status of the fetuses.....	33

Figure S28   The photo of live fetuses and placentas. ....	34
Figure S29   The H&E staining of fetuses and placentas. ....	35
<b>Supplementary Tables.....</b>	<b>36</b>
Table S1   Damage yields under X-ray irradiations for three DNA geometrical models. ....	36
Table S2   The embryonic development status in pregnant mice following injection of CBL@HfO <sub>2</sub> .....	37
Table S3   Reagents and antibodies.....	38
<b>References .....</b>	<b>39</b>

## **Experimental Section**

### **Characterization**

The TEM and EDX element mapping were obtained by using a FEI Tecnai TF20. The X-ray photoelectron spectroscopy (XPS) spectra and the surface area were recorded using a K-Alpha X-ray photoelectron spectrometer (Thermo Fisher Scientific, UK) and a Micromeritics ASAP 2460 BET apparatus, respectively, which were tested by Shiyanjia Lab ([www.Shiyanjia.com](http://www.Shiyanjia.com)). The UV-vis spectra were acquired on a UV-Vis-NIR spectrophotometer (Agilent Cary 5000, USA). The nanoparticle size was determined using a Zetasizer Nano ZS90 instrument (Malvern, UK). Fluorescence images were captured using confocal laser scanning microscopy (CLSM, A1R-si, Nikon, Japan). X-ray irradiation was conducted using an X-ray irradiator (MultiRad 160, Faxitron, USA).

### **Cell lines and animals**

All cells in this study were cultured in a medium consisting of 89% DMEM, 1% penicillin-streptomycin solution, and 10% FBS, and cultivated at 37°C with 5% CO<sub>2</sub>.

### **Simulated calculation**

The Geant4-DNA Monte Carlo (MC) toolkit was employed to investigate the conformation of DNA and the yield of DSBs induced by X-ray radiation. Geant4-DNA was utilized to calculate the yield of direct and indirect DNA damage, such as single-strand and double-strand breaks, resulting from energy deposition or interactions between DNA and free radicals. Based on the publicly available "molecule DNA" in Geant4,<sup>[1]</sup> we established a precise computational environment for simulating the irradiation of human fibroblast cells. Furthermore, different DNA geometries were constructed. The Z-DNA geometry followed a classical stacking pattern that was a common feature observed in all Z-DNA oligonucleotide crystals.<sup>[2]</sup> The geometries of A-DNA and B-DNA were established based on classical atomic coordinates and other stereochemical parameters.<sup>[3]</sup> For the MC simulation setup, we employed 1.173 MeV X-ray irradiation of cells to simulate the interaction between X-rays and cells. This included precise modeling of the physical, physicochemical, and chemical stages of liquid water irradiation, and radiolytic processes. Subsequently, the yield of SSBs and DSBs was quantified as indicators of radiation-induced damage. For each distinct DNA conformation, we

performed simulations with  $10^8$  events of X-ray.

### **Cellular uptake**

To observe intracellular uptake, the CBL@HfO<sub>2</sub> was labeled with fluorescein isothiocyanate (FITC) by overnight stirring. HCT116 cells were inoculated on the 24-well slide ( $4 \times 10^4$  per well), and cultured with treated CBL@HfO<sub>2</sub> (an equimolar concentration of CBL0137, 2.5  $\mu$ M) for 8 hours. The nuclei were stained with Hoechst. Finally, the cells were immediately observed with CLSM.

### ***In vitro* biocompatibility evaluation**

For the cell proliferation toxicity tests, we adhered to the instructions provided by the CCK-8 kit. HCT116 cells were initially seeded onto 96-well plates and allowed to incubate overnight. Subsequently, the cells were treated with HM-HfO<sub>2</sub>, CBL0137, and CBL@HfO<sub>2</sub> (an equimolar concentration of CBL0137). Following this, CCK-8 reagent was added to each well and incubated at 37 °C. The absorbance (OD) at 450 nm was measured using an enzyme-labeled instrument. For the hemolysis experiment, we extracted fresh red blood cells from BALB/c mice and prepared a suspension using PBS. The diluted red blood cell suspension was then mixed with various concentrations of HM-HfO<sub>2</sub>, CBL0137, and CBL@HfO<sub>2</sub>, and left at room temperature for 4 hours. The absorbance of the supernatant at 570 nm was measured. The PBS was used as the negative control, while deionized water served as the positive control. Hemolysis rate (%) =  $(OD_{\text{sample}} - OD_{\text{negative}}) / (OD_{\text{positive}} - OD_{\text{negative}}) \times 100\%$ .

### ***In vivo* toxicological evaluation**

Female BALB/c mice (5-6 weeks old, ~18 g each) were inoculated with CT26 cells ( $5 \times 10^4$  cells per mouse). On day 11, treatment was initiated by intratumoral injection of HM-HfO<sub>2</sub>, CBL0137, and CBL@HfO<sub>2</sub> (an equimolar concentration of CBL0137, 500  $\mu$ M, 50  $\mu$ L per mouse) or PBS for three consecutive days. The mice were closely monitored for body weight and tumor size. On the third day after the completion of treatment, major organs were harvested and subjected to H&E staining. On day 23, blood serum and whole blood were collected from the mice for biochemical and hematological analysis. To evaluate the impact after treatment of CBL@HfO<sub>2</sub> and X-ray irradiation on mice, three mice were randomly selected from each group and subjected to X-ray irradiation for localized tumors (1.5 Gy, 160 kV) after the intratumoral injection treatment. Major organs were harvested and subjected to H&E staining on the third day after irradiation.

We evaluated the impact of different concentrations of the CBL@HfO<sub>2</sub> radiosensitizer on fetal development using an ICR mouse model. The dosages of CBL@HfO<sub>2</sub> were expressed as equimolar concentrations of CBL0137, including 100 μM, 500 μM, and 1000 μM. The ICR mice were kept in cages at a ratio of 1:1 (female : male), and the vaginal suppository of female mice was checked the next morning. The day of vaginal suppository observation in the ICR female mice was designated as embryonic day 0. Pregnant mice were randomly divided into 4 groups, with 6 mice in each group. On embryonic day 5, the pregnant mice were subcutaneously injected with different concentrations of CBL@HfO<sub>2</sub> and 5% glucose solution (Control), and the injections were repeated for 3 consecutive days. The condition of the pregnant mice was continuously monitored during this period. On embryonic day 15, a cesarean section was performed to examine the developmental status of the fetal mice and placentas in each litter. Three fetal mice and their corresponding placentas from each litter were randomly selected for photography. Additionally, three fetal mice and placentas from each group were randomly chosen for histopathological examination using H&E staining.

To evaluate the impact of CBL@HfO<sub>2</sub> as a radiosensitizer on the surrounding normal tissues, 4T1 cells were implanted in the mammary glands of female BALB/c mice to establish an in-situ breast cancer model. When the tumor volume reached approximately 50 mm<sup>3</sup>, the mice received an intratumoral injection of CBL@HfO<sub>2</sub> ((an equimolar concentration of CBL0137, 500 μM) and X-ray irradiation (1.5 Gy, 160 kV), repeated consecutively for 3 days. Tumors and surrounding normal tissues were collected one day after the treatments, and tissue sections were subjected to TUNEL staining to assess the extent of damage.

---

## Supplementary Figures

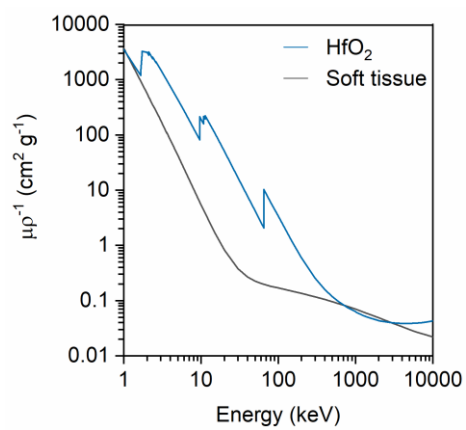


**Figure S1 | The X-ray mass attenuation coefficients of  $\text{HfO}_2$  and soft tissues.**

This was obtained from the National Institute of Standards and Technology database.

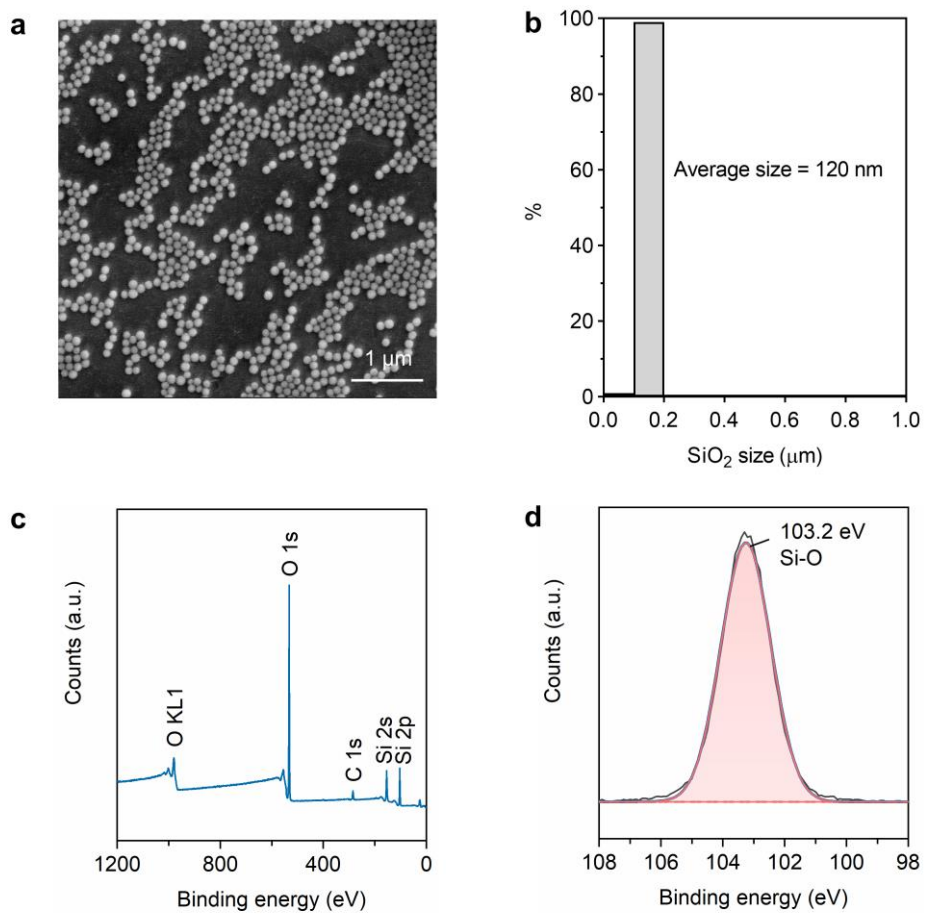


**Figure S2 | Characterization of  $\text{SiO}_2$  as a template.**

**a**, SEM image, and **b**, the average size of  $\text{SiO}_2$ . **c**, Wide and **d**, Si 2p XPS spectra of  $\text{SiO}_2$ .

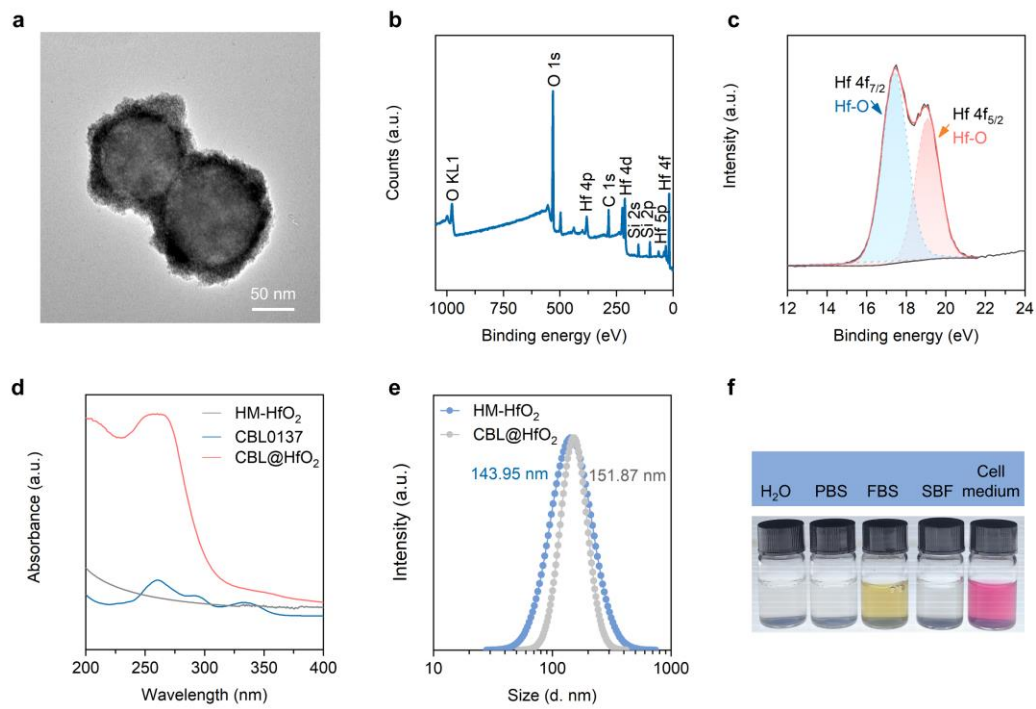


**Figure S3 | Synthesis and characterization of CBL@HfO<sub>2</sub>.**

**a**, TEM image and **b**, wide XPS of SiO<sub>2</sub>@HfO<sub>2</sub> core-shell nanospheres. **c**, Hf 4f XPS spectra of HM-HfO<sub>2</sub>. **d**, Representative UV-vis spectra of HM-HfO<sub>2</sub>, CBL0137, and CBL@HfO<sub>2</sub>. **e**, Diameter distribution of HM-HfO<sub>2</sub> and CBL@HfO<sub>2</sub>. **f**, Photograph of CBL@HfO<sub>2</sub> (500 μM) dispersed in different mediums after 24 hours.

ZOOM IN

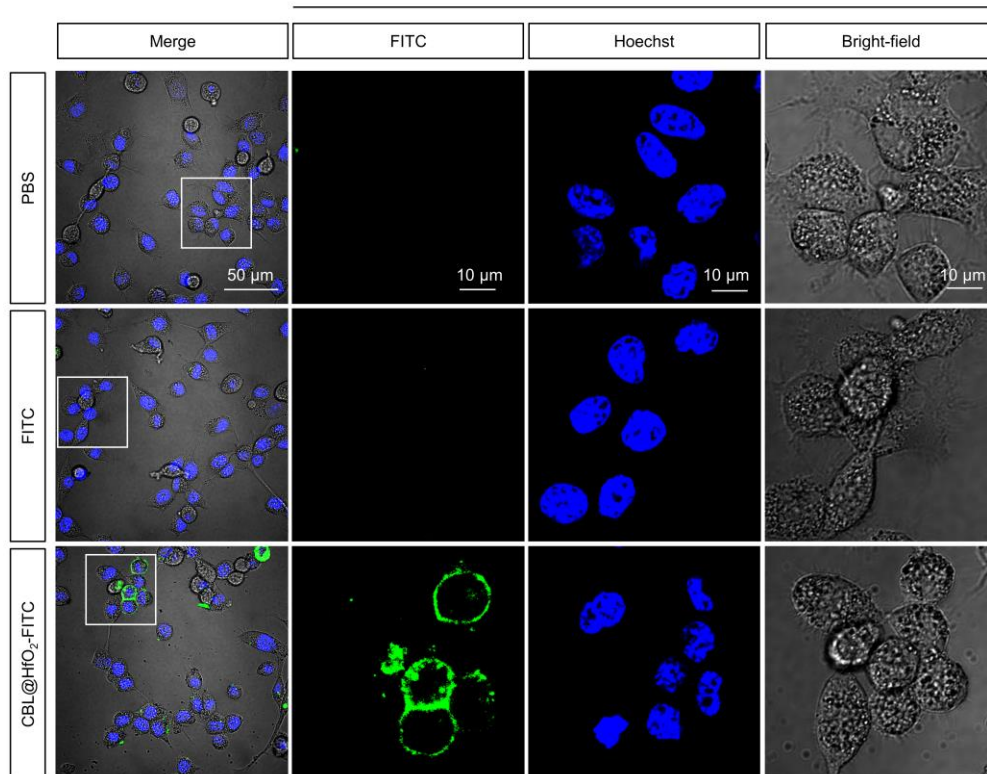


**Figure S4 | The cellular uptake behavior of CBL@HfO<sub>2</sub> after incubating for 8 hours.**

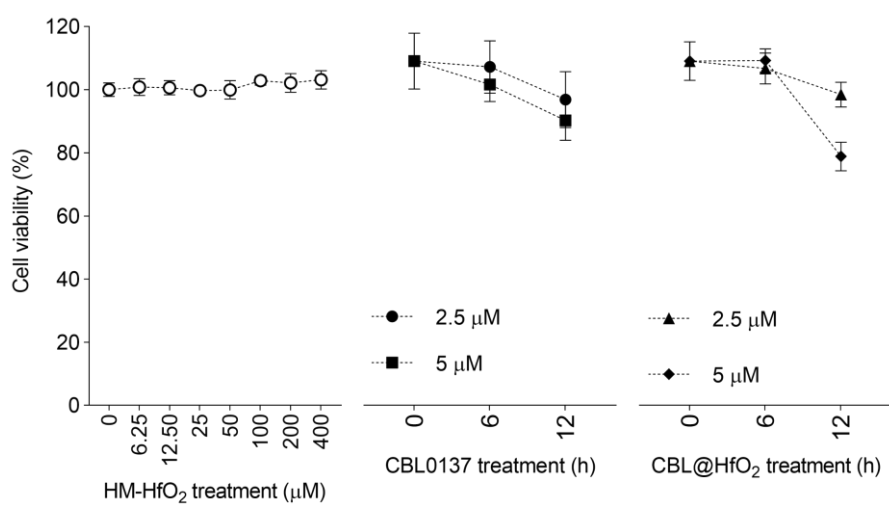


**Figure S5 | Cytotoxicity evaluation with treatments by HM-HfO<sub>2</sub>, CBL0137, and CBL@HfO<sub>2</sub>.**

Data are mean ± SD. n = 6 per group.

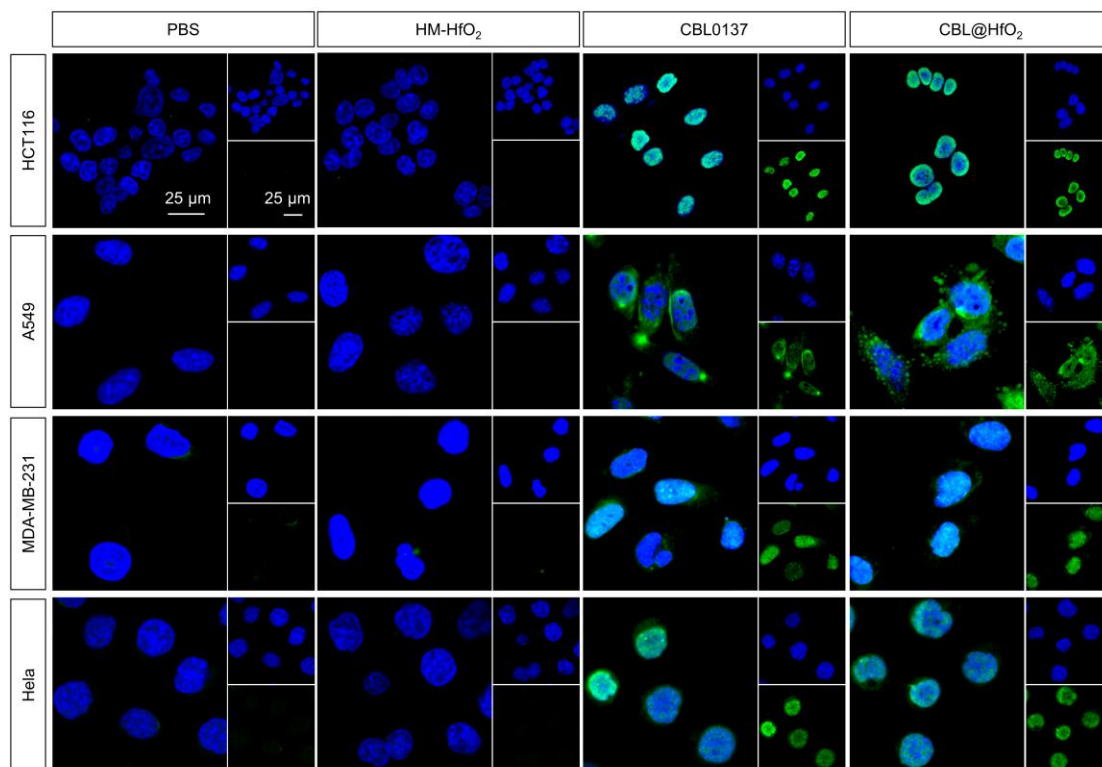


**Figure S6 | Z-DNA expression within HCT116, A549, MDA-MB-231, Hela cells.**

These cells were treated with HM-HfO<sub>2</sub>, CBL0137, and CBL@HfO<sub>2</sub> (an equimolar concentration of CBL0137, 5 μM).

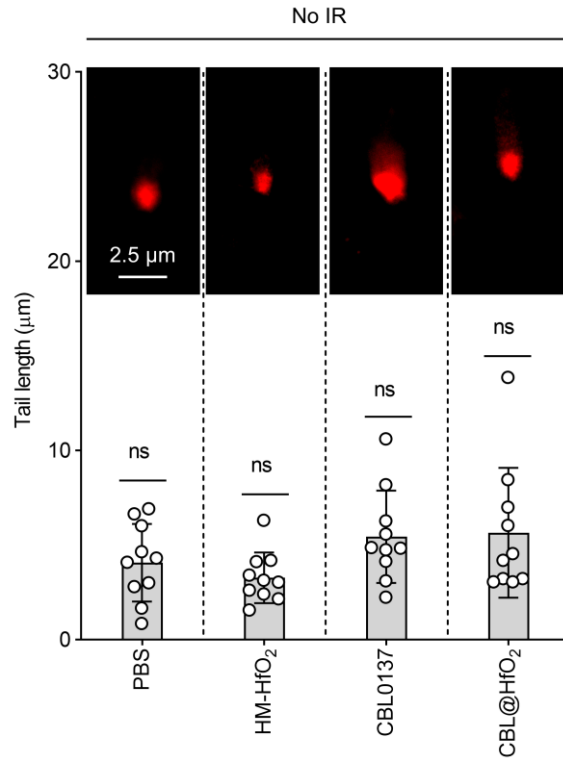


**Figure S7 | Comet assay of HCT116 cells with treatment.**

These cells were treated with HM-HfO<sub>2</sub>, CBL0137, and CBL@HfO<sub>2</sub> for 8 hours (an equimolar concentration of CBL0137, 5 μM). Data are mean ± SD. n = 10 per group. Ordinary one-way analysis of variance (ANOVA).

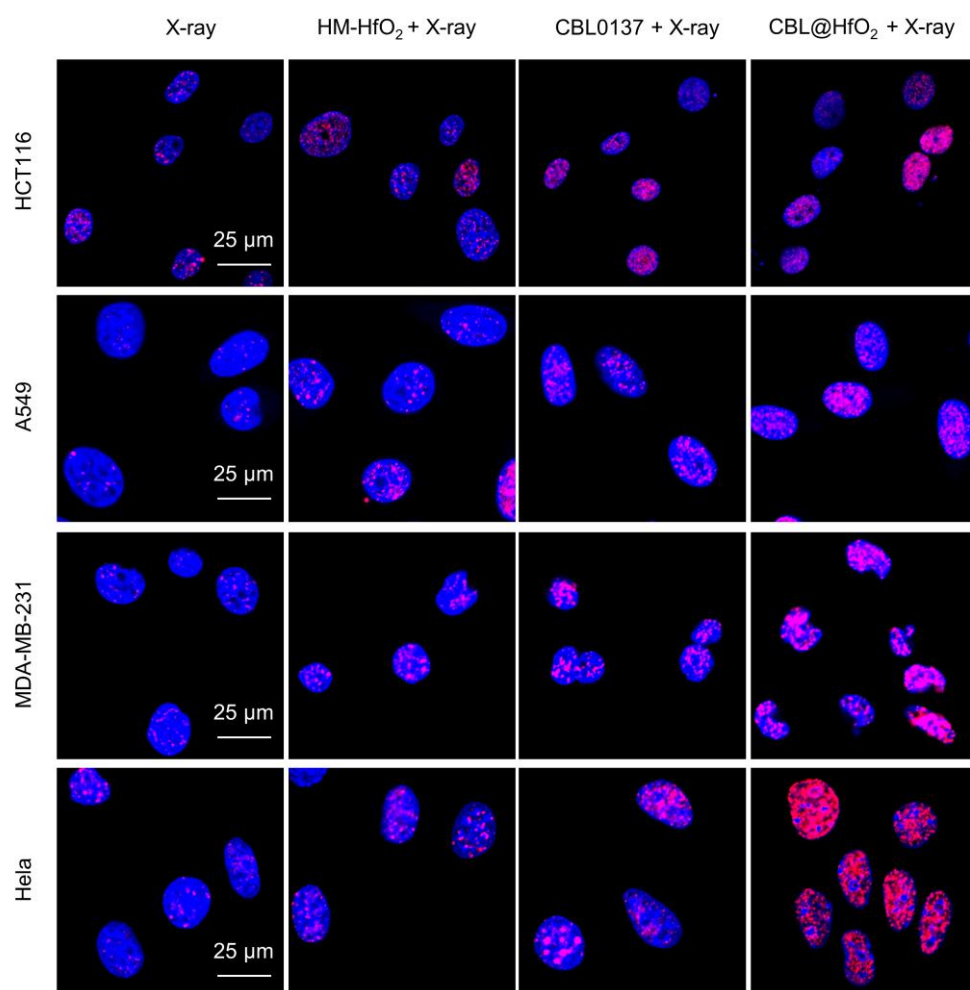


**Figure S8 | The  $\gamma$ H2AX expression within HCT116, A549, MDA-MB-231, and HeLa cells.**  
 These cells were treated by HM-HfO<sub>2</sub>, CBL0137, and CBL@HfO<sub>2</sub> (an equimolar concentration of CBL0137, 5  $\mu$ M) and subsequently X-ray irradiation (4 Gy).

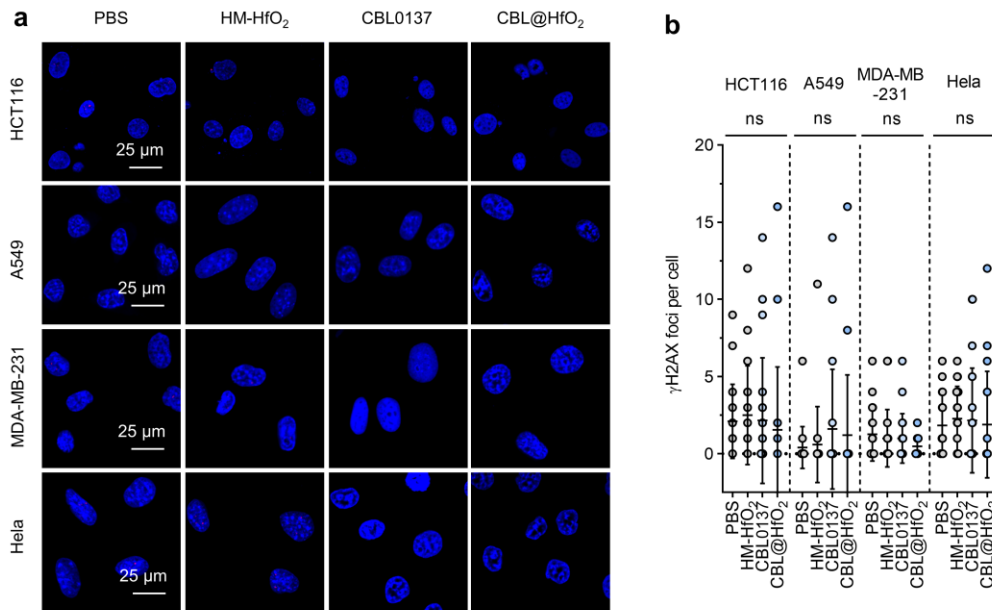


**Figure S9 | The  $\gamma$ H2AX expression within HCT116, A549, MDA-MB-231, and HeLa cells.**  
**a**, Representative immunofluorescence images, and **b**, corresponding analysis. These cells were treated by HM-HfO<sub>2</sub>, CBL0137, and CBL@HfO<sub>2</sub> (an equimolar concentration of CBL0137, 5  $\mu$ M). Data are mean  $\pm$  SD. n = 10 per group. Ordinary one-way analysis of variance (ANOVA).

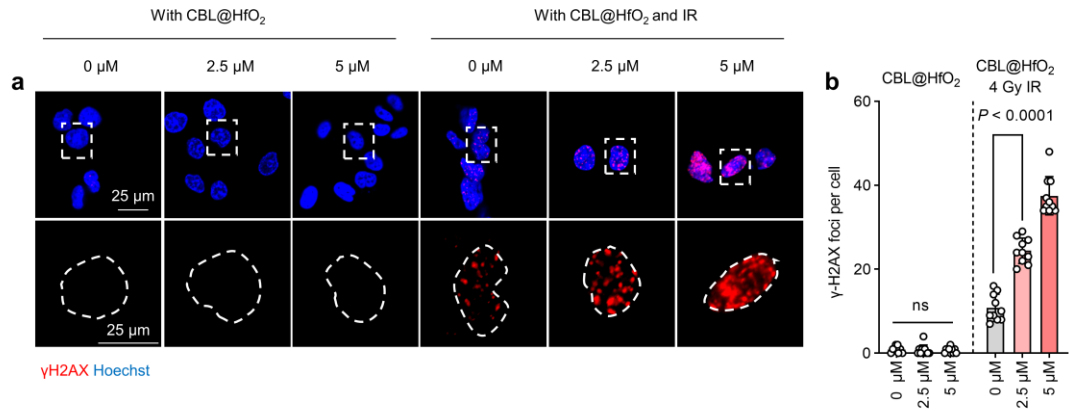


**Figure S10 | The  $\gamma$ H2AX expression within HCT116 cells after different treatments.**

**a**, The representative immunofluorescence images, and **b**, the quantization of mean fluorescence intensity. The cells were treated by CBL@HfO<sub>2</sub> (an equimolar concentration of CBL0137, 2.5  $\mu$ M and 5  $\mu$ M) and subsequently X-ray irradiation (4 Gy). Data are mean  $\pm$  SD. n = 10 per group. Ordinary one-way analysis of variance (ANOVA).

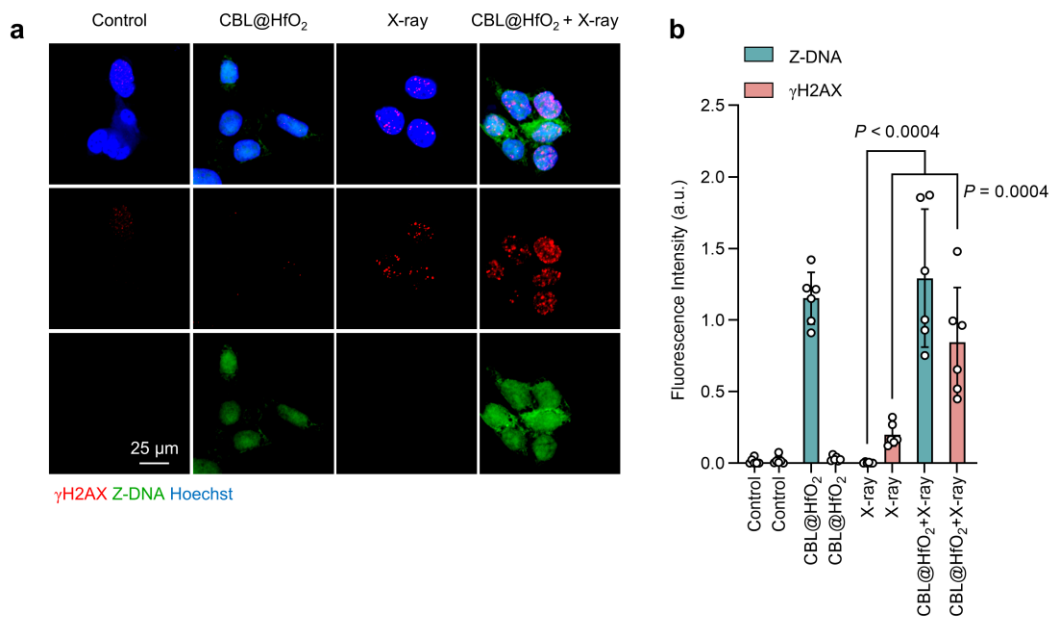


**Figure S11 | The co-staining of  $\gamma$ H2AX and Z-DNA within HCT116 cells after treatments.**

**a**, The representative immunofluorescence images, and **b**, the quantization of mean fluorescence intensity. The cells were treated by CBL@HfO<sub>2</sub> (an equimolar concentration of CBL0137, 5 μM) and subsequently X-ray irradiation (4 Gy). Data are mean ± SD. n = 6 per group. Ordinary one-way analysis of variance (ANOVA).

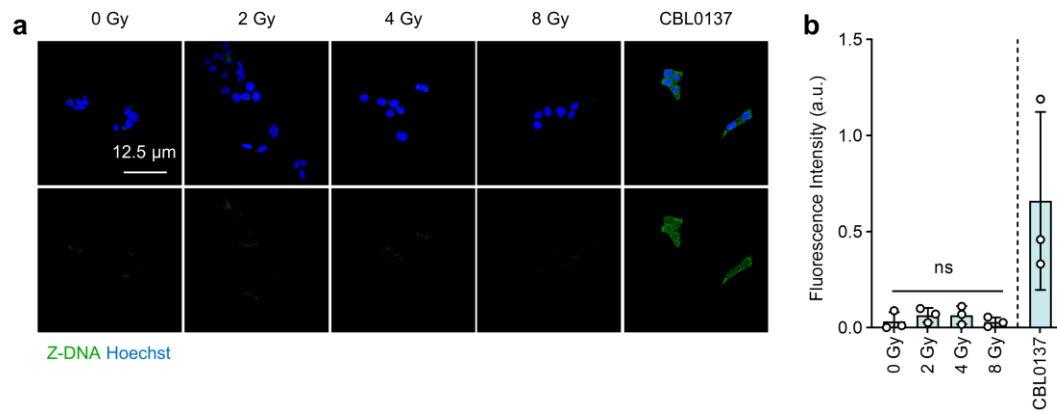


**Figure S12 | The Z-DNA expression within HCT116 cells after different doses of irradiation.** **a**, Representative immunofluorescence images representing Z-DNA, and **b**, the corresponding quantization. Cells in the positive group were treated with CBL0137 alone for 8 hours (5  $\mu$ M). Data are mean  $\pm$  SD. n = 3 per group. Ordinary one-way analysis of variance (ANOVA).

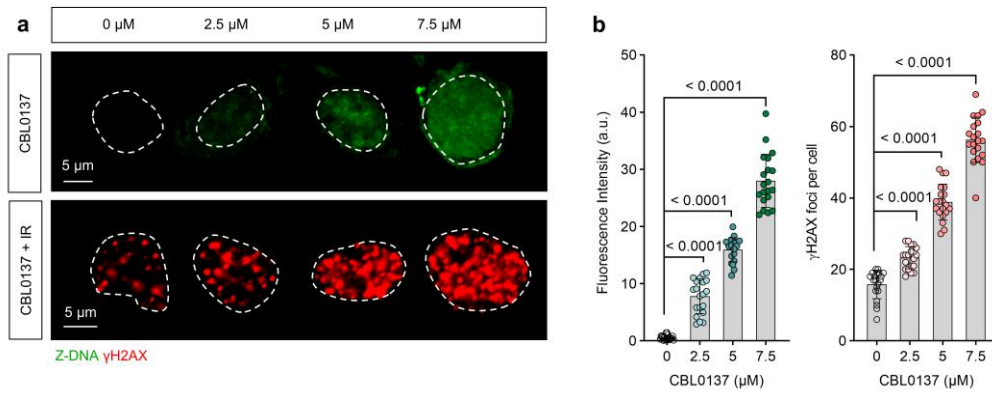


**Figure S13 | The  $\gamma\text{H2AX}$  and Z-DNA expression within HCT116 cells after treatment with different concentrations of CBL0137.**

**a**, Fluorescence images, and **b**, corresponding analysis. Data are mean  $\pm$  SD.  $n = 20$  per group. Ordinary one-way analysis of variance (ANOVA).

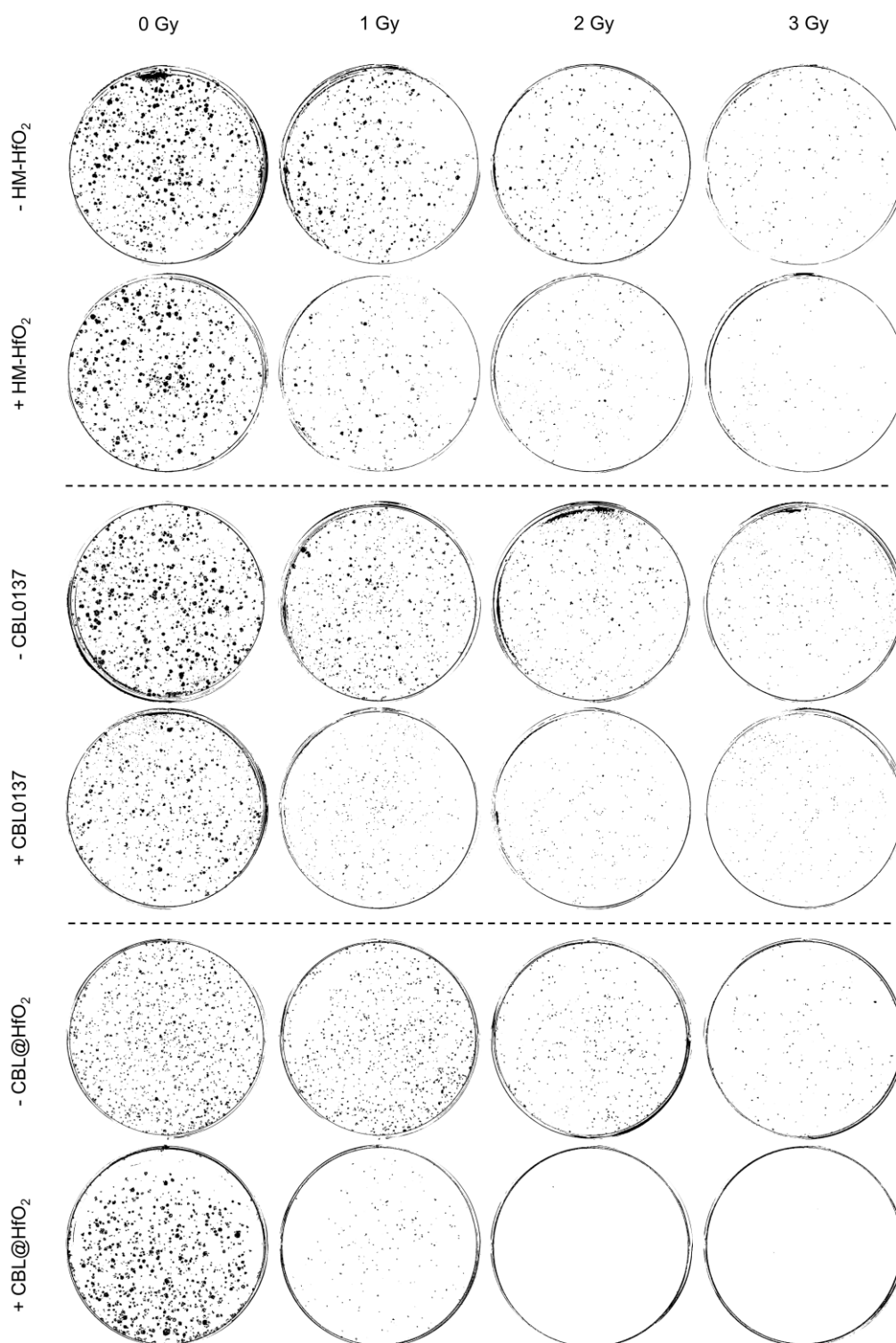


**Figure S14 | Colony formation of HCT116 cells treated with HM-HfO<sub>2</sub>, CBL0137, and CBL@HfO<sub>2</sub>.**

The equimolar concentration of CBL0137 (0.5 μM) with incubation for 8 hours and subsequent IR irradiation (160 kV) was employed.

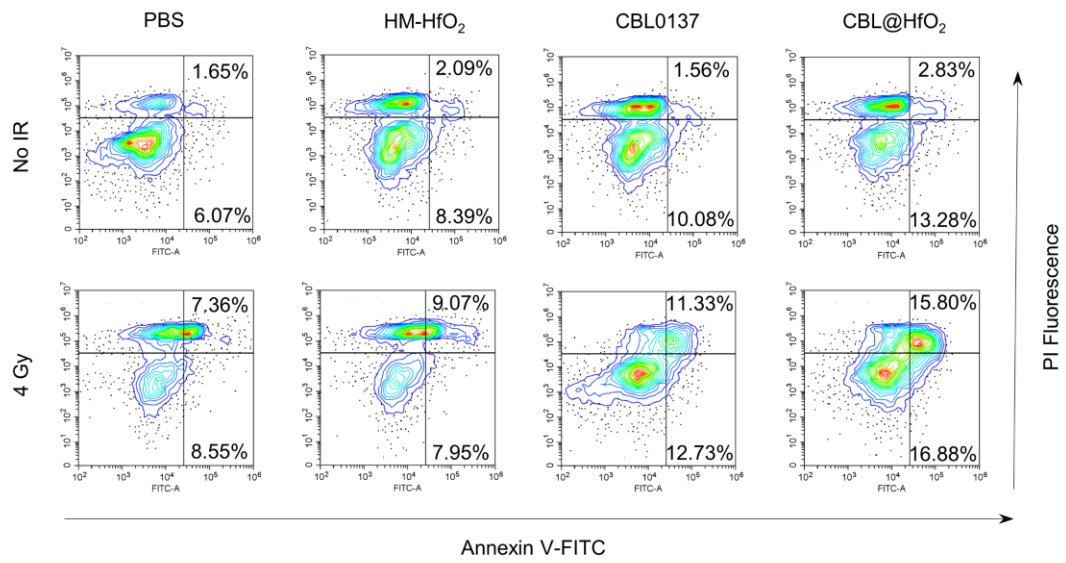


**Figure S15 | Cell death evaluation of HCT116 cells after treatments.**

HCT116 cells were treated with HM-HfO<sub>2</sub>, CBL0137, and CBL@HfO<sub>2</sub> (an equimolar concentration of CBL0137, 2.5 μM) and subsequent X-ray irradiation (4 Gy).

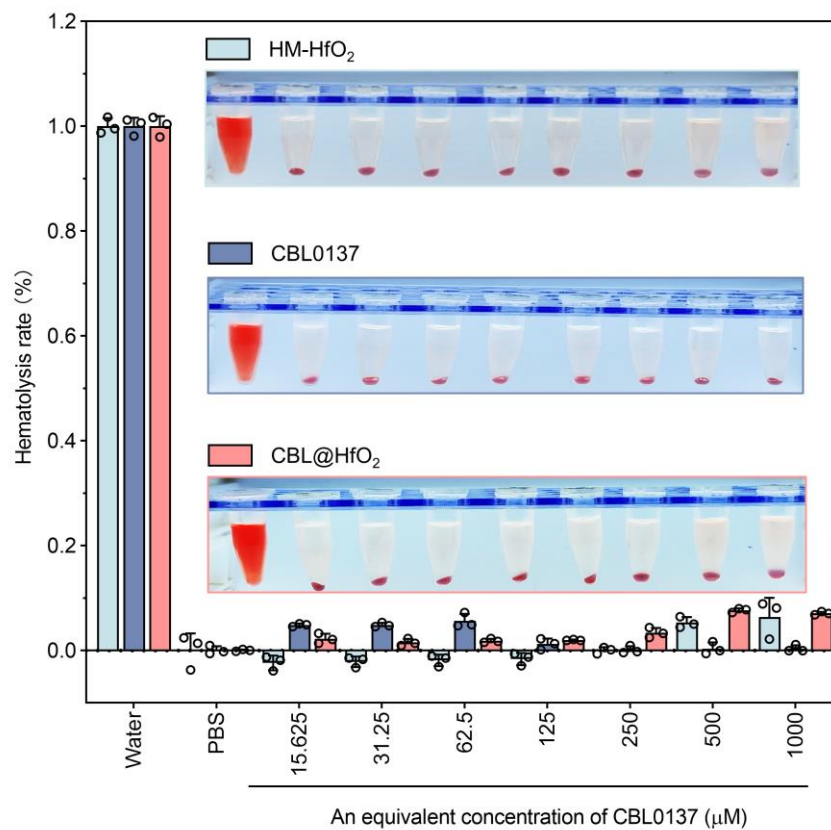


**Figure S16 | Hemolysis assay of HM-HfO<sub>2</sub>, CBL0137, and CBL@HfO<sub>2</sub>.**  
Data are mean ± SD. n = 3 per group.

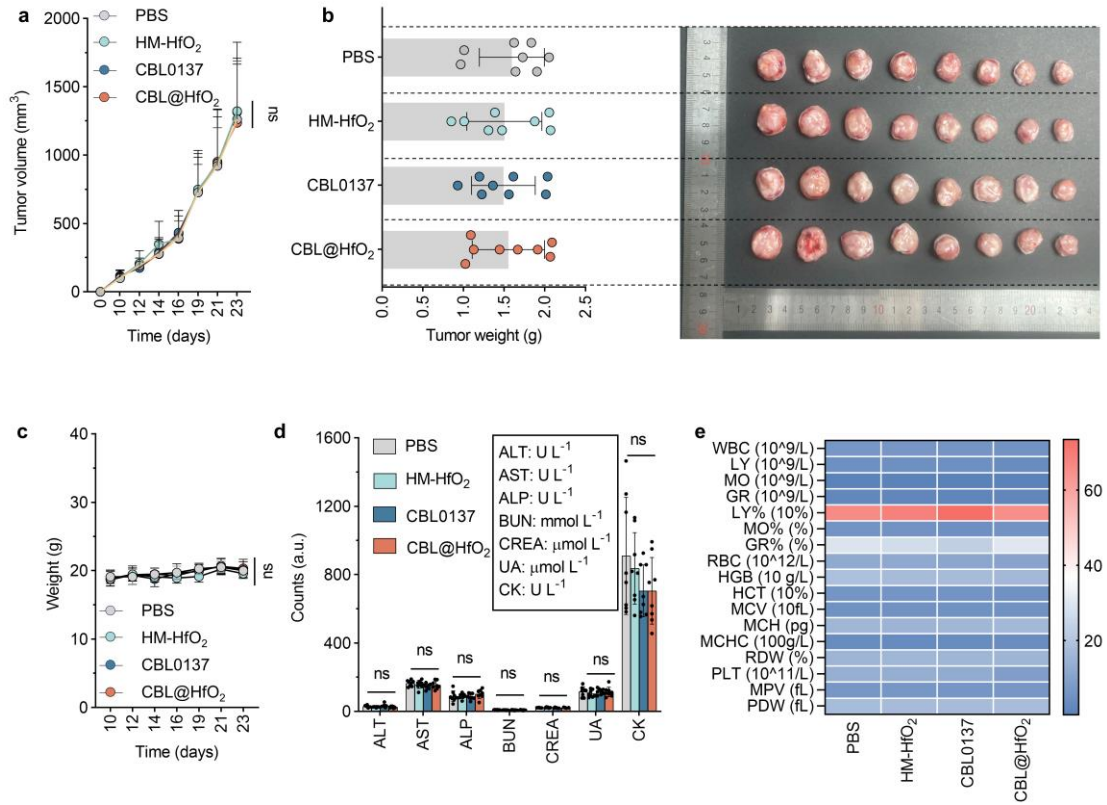


**Figure S17 | *In vivo* toxicological evaluation.**

The monitoring of **a**, tumor volume, **b**, tumor weight, and tumor size of the treatment endpoint. **c**, Body weight curves of mice consecutively treated with PBS (control), HM-HfO<sub>2</sub>, CBL0137, and CBL@HfO<sub>2</sub> (an equimolar concentration of CBL0137, 500 μM) for 3 times. **d**, Hematological parameters, and **e**, blood biochemistry of CT26 tumor-bearing mice. All experiments are biologically independent. Data are mean ± SD. n = 8 per group in **a-c**. n = 3 per group in **d, e**. Ordinary one-way analysis of variance (ANOVA).

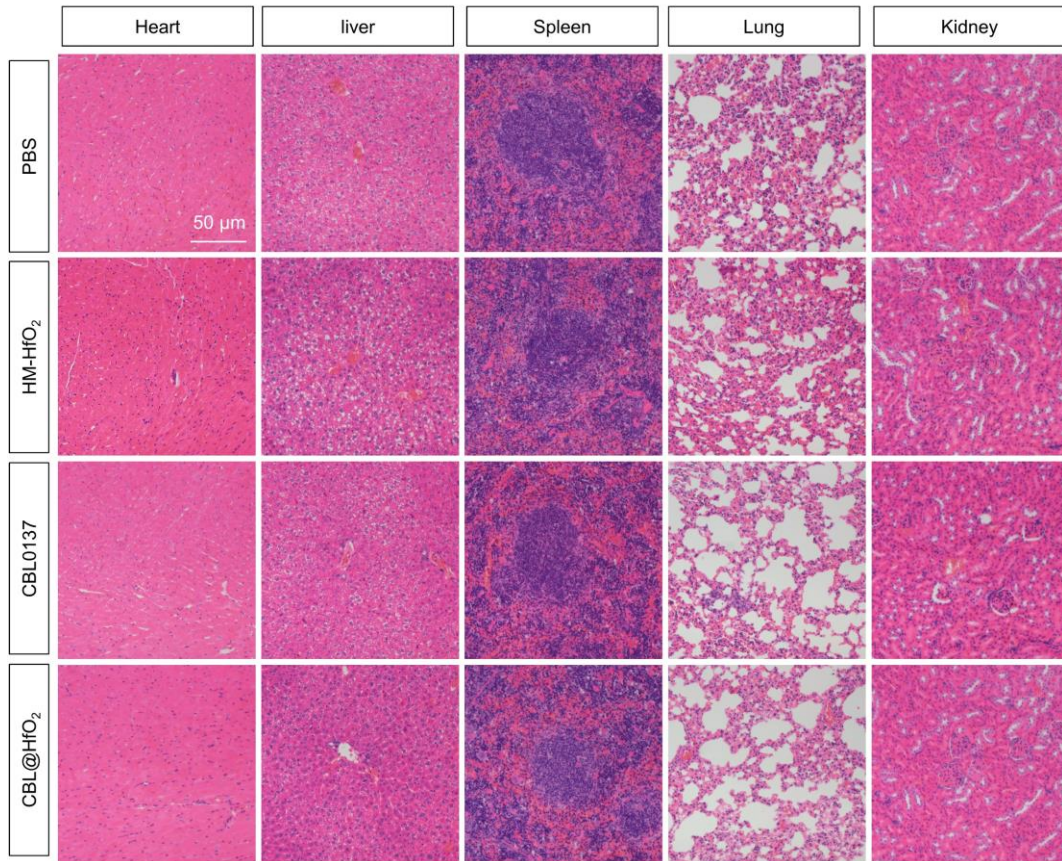


**Figure S18 | Histologic sections of major organs with intratumoral treatment.**

The CT26 tumor-bearing mice were treated with HM-HfO<sub>2</sub>, CBL0137, and CBL@HfO<sub>2</sub> (an equimolar concentration of CBL0137, 500 μM).

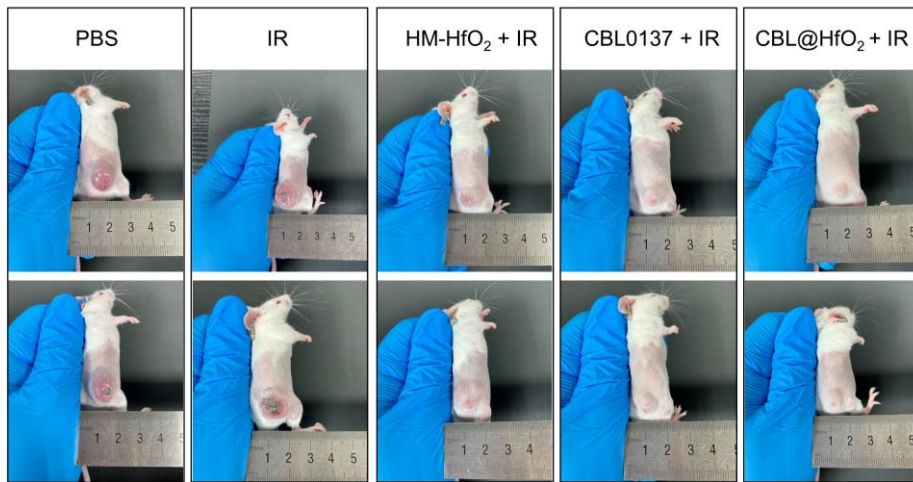


**Figure S19 | Photographs of mice after treatment at day 30.**

Tumour regression after treatment, CR = 3/10



**Figure S20 | Photographs of tumor regression.**

Among the 10 mice in the CBL@HfO<sub>2</sub> + IR group, tumor regression was observed in 3 mice, 30% of the tumors were in complete response (CR), and no tumor recurrence was observed at day 60.

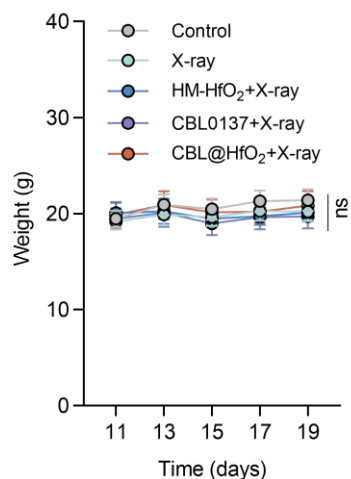


**Figure S21 | Body weight curves of mice with treatments.**

The mice were consecutively treated with HM-HfO<sub>2</sub>, CBL0137, and CBL@HfO<sub>2</sub> (an equimolar concentration of CBL0137, 500  $\mu$ M) and subsequent X-ray irradiation (1.5 Gy, 160 kV) for 3 times. All experiments are biologically independent. Data are mean  $\pm$  SD. n = 10 per group. Ordinary one-way analysis of variance (ANOVA).

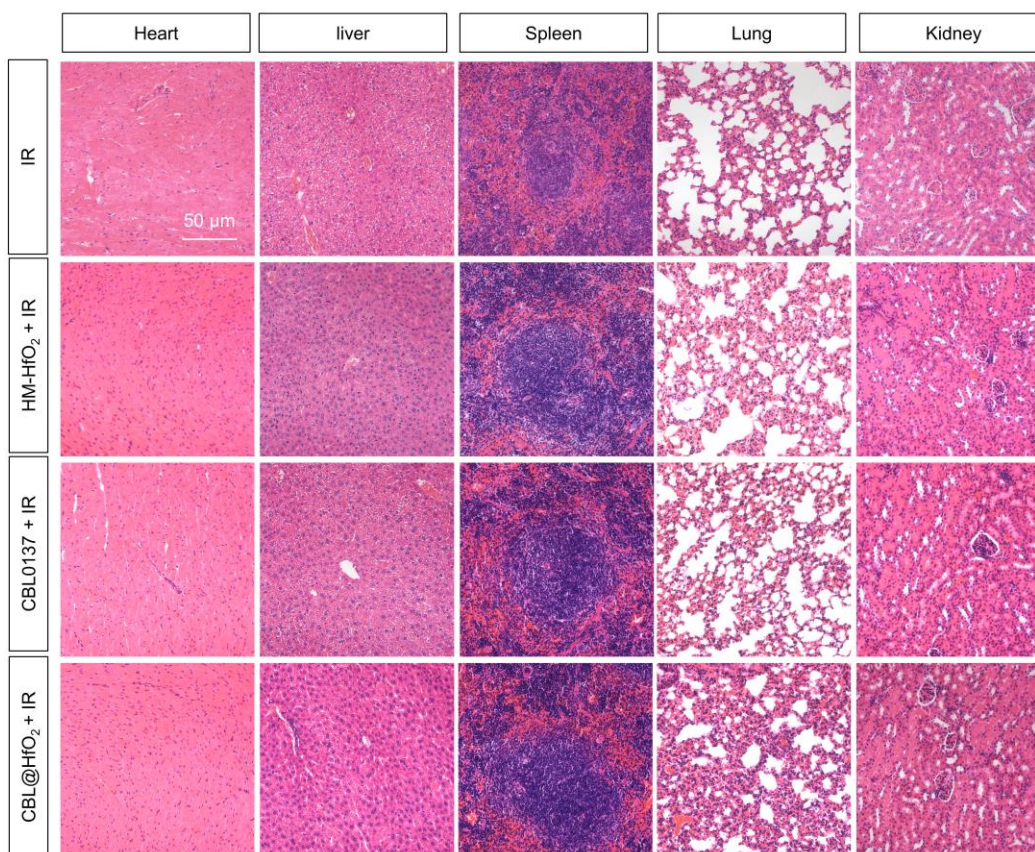


**Figure S22 | Histologic sections of major organs with intratumoral treatment and subsequent IR irradiations.**

These mice were treated by HM-HfO<sub>2</sub>, CBL0137, and CBL@HfO<sub>2</sub> (an equimolar concentration of CBL0137, 500 μM) and subsequent IR irradiations (1.5 Gy, 160 kV).

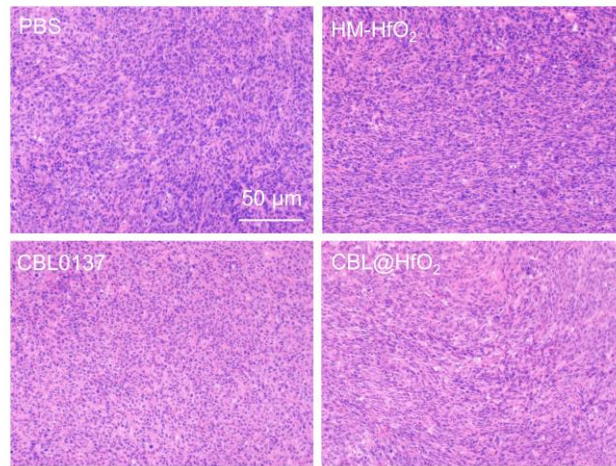


**Figure S23 | Expression of H&E in tumor sections.**

The tumors were treated by HM-HfO<sub>2</sub>, CBL0137, and CBL@HfO<sub>2</sub> (an equimolar concentration of CBL0137, 500 μM). No significant difference in H&E expression was observed for these treated tumors.

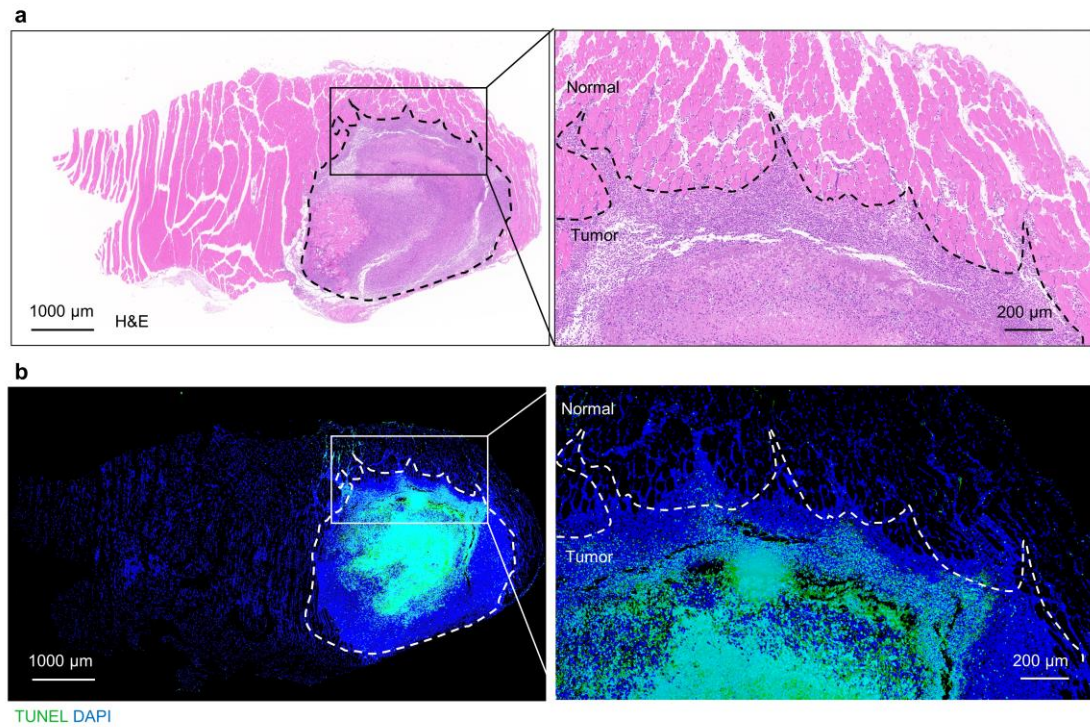


**Figure S24 | Damage analysis of tumor and peritumoral normal tissue after CBL@HfO<sub>2</sub> and IR treatment.**

**a**, H&E, and **b**, TUNEL staining of tumor and peritumoral normal tissue. The mice were administered with the radiosensitizer CBL@HfO<sub>2</sub> (an equimolar concentration of CBL0137, 500 μM) via intratumoral injection, followed by local tumor irradiation (1.5 Gy, 160 kV) 6 hours later, and repeated for three consecutive days. Tumors and surrounding normal tissues were collected for histological examination one day after the treatment.

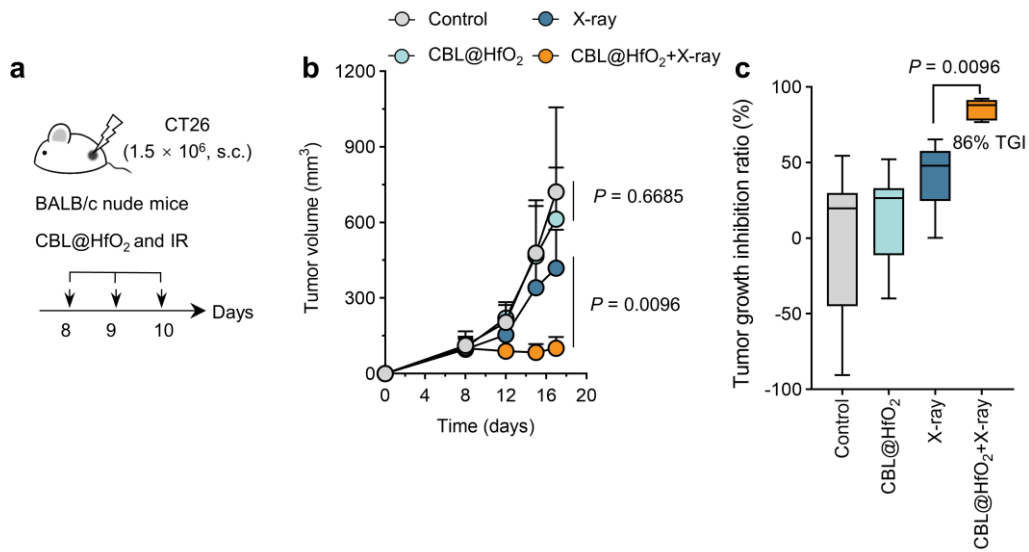


**Figure S25 | *In vivo* radiosensitization based on CBL@HfO<sub>2</sub> nanocapsule.**

**a**, The treatment process of subcutaneous CT26 tumor model in nude mice. **b**, The growth kinetics, and **c**, tumor growth inhibition (TGI) rate of tumors. The nude mice were intratumorally injected with CBL@HfO<sub>2</sub> (an equimolar concentration of CBL0137, 500 μM) and subsequently irradiated (1.5 Gy, 160 kV) for three consecutive days. All experiments are biologically independent. All data are expressed as mean ± SD. n = 10 per group. Ordinary one-way analysis of variance (ANOVA).

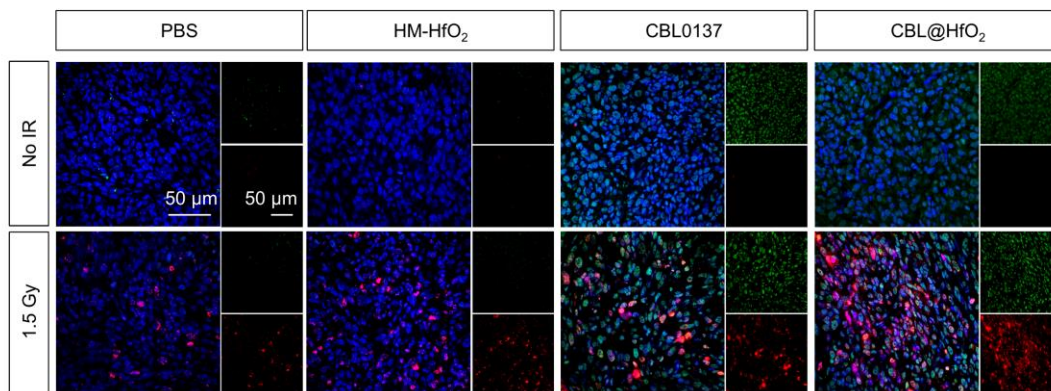


**Figure S26 | The  $\gamma$ H2AX and Z-DNA expression within CT26 tumor sections.**

The tumors were treated with HM-HfO<sub>2</sub>, CBL0137, and CBL@HfO<sub>2</sub> (an equimolar concentration of CBL0137, 500  $\mu$ M) and subsequent IR irradiations (1.5 Gy, 160 kV). The treatment was repeated for three consecutive days.

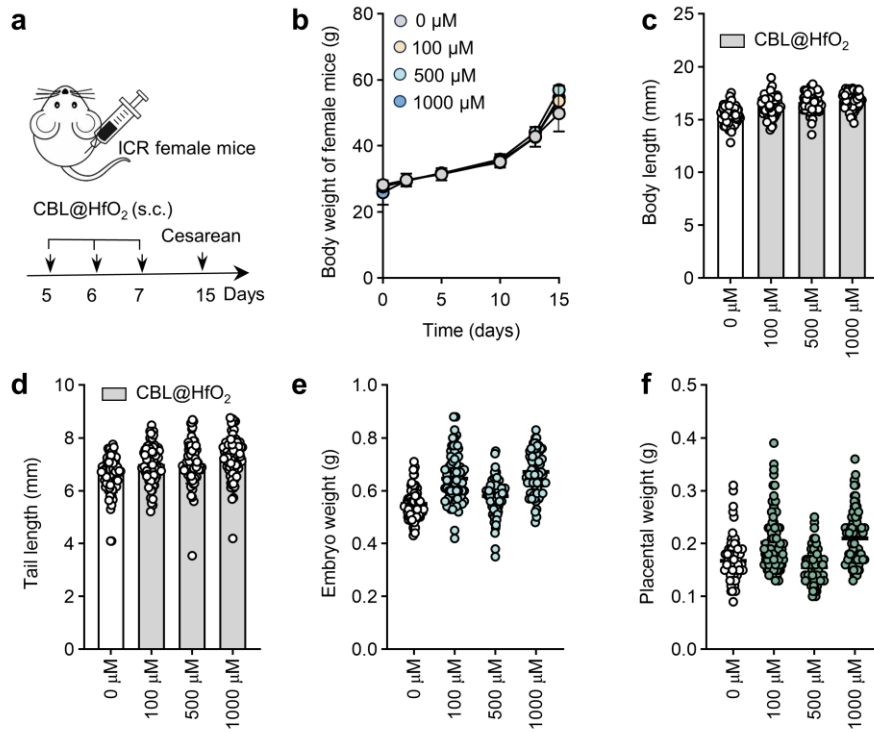


**Figure S27 | Developmental status of the fetuses.**

**a**, Experimental procedure diagram. **b**, Body weight of female mice. **c**, Body length, and **d**, tail length of live fetuses. **e**, Embryo weight. **f**, Placental weight. All experiments are biologically independent. All data are expressed as mean  $\pm$  SD.  $n = 6$  per group in **b**. The data in **c-f** are from all live fetuses and placentas.



**Figure S28 | The photo of live fetuses and placentas.**

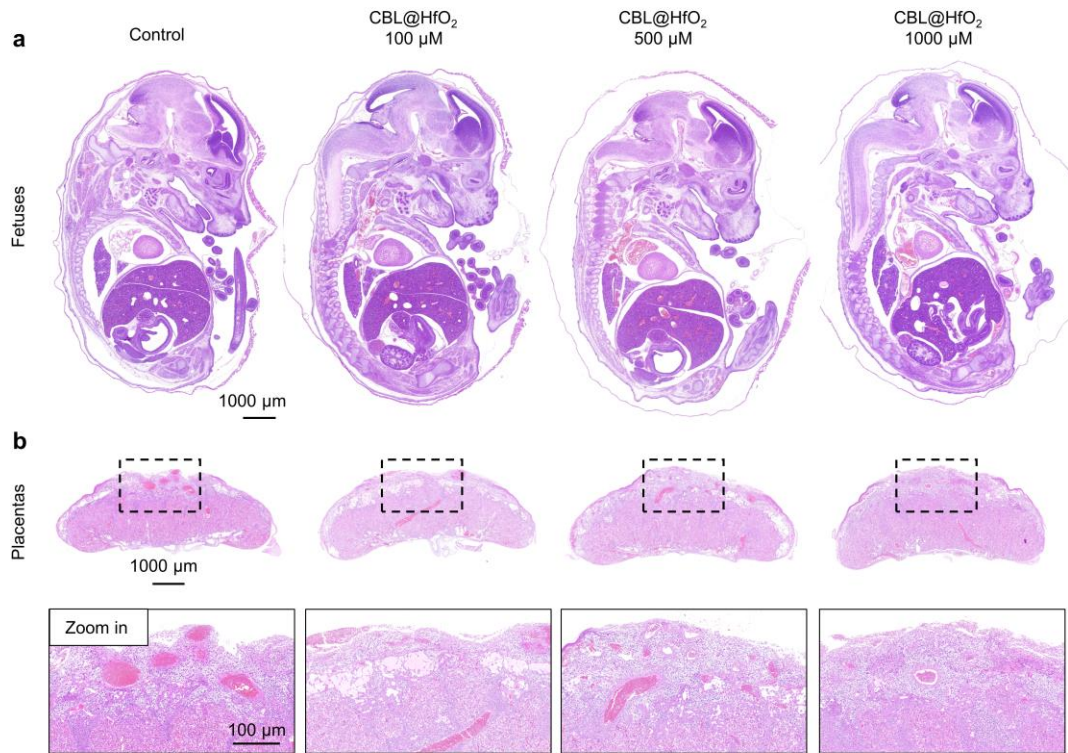


**Figure S29 | The H&E staining of fetuses and placentas.**

Histological examination of **a**, live fetuses and **b**, placentas after administration of CBL@HfO<sub>2</sub> nanosensitizer.

## Supplementary Tables

**Table S1 | Damage yields under X-ray irradiations for three DNA geometrical models.**

DNA conformation	SSB (Gy <sup>-1</sup> Gbp <sup>-1</sup> )	DSB (Gy <sup>-1</sup> Gbp <sup>-1</sup> )	SSB/DSB
A-DNA	86.1313	4.41699	19.5
B-DNA	103.446	4.70208	22
Z-DNA	102.567	7.32619	14

**Table S2 | The embryonic development status in pregnant mice following injection of CBL@HfO<sub>2</sub>.**

Observation parameters	Dosage (an equimolar concentration of CBL0137)			
	0	100 $\mu$ M	500 $\mu$ M	1000 $\mu$ M
Litter size	14.5 $\pm$ 1.8	14 $\pm$ 3.8	15.3 $\pm$ 1.8	13.3 $\pm$ 0.5
Total live fetuses	84	83	92	78
Total stillbirths	0	1	0	1
Total resorptions	3	0	0	0

**Table S3 | Reagents and antibodies.**

<b>Chemical reagent</b>	<b>Company</b>	<b>Purity</b>
C <sub>16</sub> H <sub>36</sub> O <sub>4</sub> Hf (70% in n-butanol)	Beijing Forssman Technology Co., LTD	Hf, 26 wt. %
Tetraethyl orthosilicate (TEOS)	Beijing Innochem Technology Co., LTD	≥ 99.0%
NaOH	Beijing Innochem Technology Co., LTD	AR
Ammonia solution	Beijing Innochem Technology Co., LTD	25.0-30.0%
Acetonitrile	Beijing Innochem Technology Co., LTD	≥99.9%
Ethanol absolute	Beijing Innochem Technology Co., LTD	99.5%
Agarose	Maclin Biochemical Technology Co., LTD	M
Low melting agarose	Maclin Biochemical Technology Co., LTD	-
CBL0137 hydrochloride	MedChemExpress	99.66%
FBS	Zhejiang Meisen Cell Technology Co., LTD	-
Penicillin-streptomycin	Dalian Meilun Biotechnology Co., LTD	-
Paraformaldehyde	Biosharp	4%
Tryptanthrin	Dalian Meilun Biotechnology Co., LTD	-
DMEM	Gibco	-
PBS	Servicebio	-
Annexin V/FITC	Dojindo	-
Cell Counting Kit-8	Dojindo	-
Hoechst 33342	Dojindo	-
Anti-Z-DNA (Z22)	Absolute Antibody Co., LTD	-
Phospho-Histone H2A.X (Ser139)	Cell Signaling Technology Co., LTD	-
TUNEL	Servicebio	-
H&E	Servicebio	-

## References

- [1] K. P. Chatzipapas, N. H. Tran, M. Dordevic, S. Zivkovic, S. Zein, W. G. Shin, D. Sakata, N. Lampe, J. M. C. Brown, A. Ristic-Fira, I. Petrovic, I. Kyriakou, D. Emfietzoglou, S. Guatelli, S. Incerti, *Precis. Radiat. Oncol.* **2023**, 7, 4.
- [2] C. Sadasivan, N. Gautham, *J. Mol. Biol.* **1995**, 248, 918.
- [3] S. Arnott, D. W. L. Hukins, *Biochem. Biophys. Res. Commun.* **1972**, 47, 1504.